

# Image analysis of Mitochondrial Texture in Progeria patients in response to shear stress and nuclear segmentation

Emily Speranza

April 3, 2013

Director:  
Kelly Cline


Readers:  
Phil Rose  
Stefanie Otto-Hitt  
Virginia Cooper

## **Abstract**

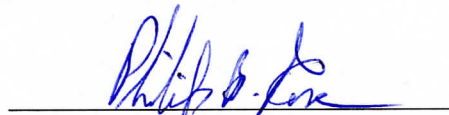
In this paper, the effects of Hutchinson-Gilford progeria syndrome on endothelial cell's mitochondrial response to shear stress will be discussed. I will also be addressing nuclear texture and differences in these same patient cells as compared to healthy cell lines. To accomplish this, I used cell culturing and fluorescent imaging techniques to gather images of cells to analyze the application of shear stress. I then used the Image Toolbox in Matlab to develop and implement a segmentation algorithm for these cells and ran analysis processes on them. Segmentation processes for the mitochondrial material and nuclear material were then developed. After segmentation, images were run through programs to perform Linear Optimal Transportation (LOT) analysis and some basic statistical tests. I found that after application of low shear stress for one hour, there was a spike in the amount of unhealthy mitochondria present. This returned to normal levels between one and six hours later. In the cells with the HGPS mutation, after the application of high shear stress, the mitochondria failed to recover and continued to show increases in the amount of unhealthy mitochondria. Differential clumping patterns of the unhealthy mitochondria were also observed in the HGPS cells as they gathered near the nucleus in larger clumps. Collectively, these results suggest that the endothelial cells of HGPS patients struggle to excrete the mitochondrial material.

SIGNATURE PAGE


This thesis for honors recognition has been approved for the  
Department of: Math, Engineering, and Computer Science.

  
\_\_\_\_\_  
Director: Dr. Kelly Cline

4/2/13  
Date

  
\_\_\_\_\_  
Reader: Phil Rose

4/2/13  
Date

  
\_\_\_\_\_  
Reader: Dr. Stefanie Otto-Hitt

4/2/13  
Date

---

# Contents

<b>1</b>	<b>Introduction</b>	<b>4</b>
1.1	Hutchinson-Gilford progeria syndrome . . . . .	4
1.2	Molecular Basis for the Disease . . . . .	4
1.2.1	Lamin A . . . . .	5
1.2.2	Progeria Protein . . . . .	6
1.3	Cell Physiology of Progeria . . . . .	7
1.4	Image Analysis . . . . .	8
1.4.1	Imaging of Cells . . . . .	8
1.4.2	Segmentation . . . . .	10
1.4.3	Analysis . . . . .	11
1.5	Overview of Project . . . . .	11
<b>2</b>	<b>Materials &amp; Methods</b>	<b>11</b>
2.1	Cell lines . . . . .	11
2.2	Application of Shear Stress . . . . .	12
2.3	Staining and Imaging . . . . .	13
2.4	Segmentation of Images and Processing . . . . .	14
2.4.1	Development of the Segmentation Algorithm . . . . .	14
2.5	Post Segmentation Analysis . . . . .	17
<b>3</b>	<b>Results</b>	<b>18</b>
3.1	Segmentation . . . . .	18
3.2	Ratio Results . . . . .	19
3.3	LOT and PCA Analysis . . . . .	20
<b>4</b>	<b>Discussion</b>	<b>21</b>
4.1	Segmentation Algorithms . . . . .	21
4.2	Ratio Tests . . . . .	23
4.3	LOT Analysis . . . . .	24
<b>5</b>	<b>Conclusion</b>	<b>25</b>
<b>6</b>	<b>Acknowledgments</b>	<b>26</b>

# 1 Introduction

## 1.1 Hutchinson-Gilford progeria syndrome

Hutchinson-Gilford progeria syndrome, or HGPS, is a genetic disorder caused by a point mutation in the *LMNA* gene which produces the lamin A protein [9]. This disease has profound effects. HGPS is associated with premature aging, and is used as a model for studying aging [5]. Children with the disease have an average life expectancy of 13 years and usually die from cardiovascular disease associated with myocardial infarction (heart attack) or stroke due to an altered response to shear stress in their endothelial cells [3] [4]. Tissues most affected by the disease are ones that are subjected to large amounts of mechanical stress, mostly structural tissues such as the cells lining the blood vessels or in the skin. These tissues fail to respond in a healthy way to mechanical stress and will die quicker than a healthy cell [11] [12]. This mutation can also be seen to accumulate naturally throughout a person's lifetime [8].

HGPS is a very uncommon disease. It is estimated that only 1 in 4 million babies are born with it worldwide each year. Since the disease was first discovered in 1886, there have only been 130 case studies in the literature. Children born with the disease will appear to grow normally for the first year of life. After their first year, the children will start to show signs of aging including extensive hair loss, vision problems, joint problems and loss of subcutaneous fat causing the appearance of wrinkled skin [10].

## 1.2 Molecular Basis for the Disease

HGPS is caused by a single nucleotide mutation in the *LMNA* gene [10]. This mutation leads to an alternate splice site in the mRNA produced by the gene resulting in an exon being spliced out. During translation of the mRNA, there is a 50 amino acid missing sequence normally encoded by the missing exon. This truncated section dis-

rupts normal function of the protein and the normal splicing of the pre-lamin protein which leads to production of a malfunctioning protein. The malfunctioning protein will fail to disconnect from the nuclear envelope and fail to enter into the center of the nucleus [5] [11].

### 1.2.1 Lamin A

The lamin A protein is a member of the Lamin protein family which provide structural support and organization to the nucleus. It is produced by the *LMNA* gene [2] [1]. These proteins help to prevent nuclear deformations and keep chromosomes in their respective areas. Contrary to popular belief, the nucleus is a highly organized structure, and when the organization is thrown off, it can have profound effects throughout the whole cell. The genes within the nucleus that need to be transcribed together are often kept within transcription “hot” regions. These regions show larger amounts of uncondensed chromosomes and are specialized to collect transcription factors and other proteins important in transcription. Genes that are most important in maintaining homeostasis within the cell are usually found in these regions, whereas other genes are found near the nuclear periphery [5].

There are two important lamin proteins found in the eukaryotic cell nucleus, lamin A and lamin B. Lamin B proteins usually remain partially embedded within the nuclear envelope and provide an underlying structure for the envelope [2]. Lamin A proteins are initially embedded within the nuclear envelope, however after maturation of the protein, lamin A will detach and enter into the central area of the nucleus [2] [8]. These proteins will then go on to provide scaffolding for the genetic material within the nucleus and help to structure the chromosomes. They are vital in making sure that the right chromosomes and the right chromosomal regions are positioned properly within in the nucleus [5].

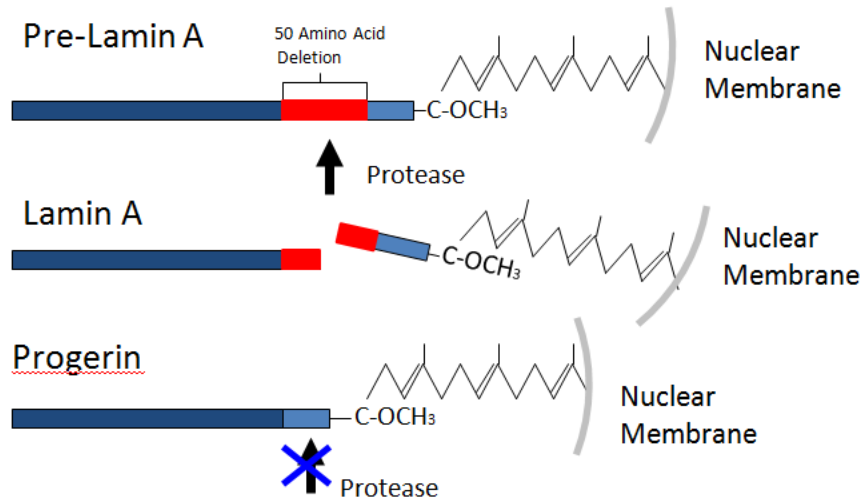


Figure 1: The post processing of the lamin A protein allowing it to detach from the nuclear envelope with the help of a protease. In the wild type protein, the red region has a splice site for the protease and will detach. In the Progeria protein, the 50 amino acid red sequence that contains the splice site is missing and the protease cannot splice the protein. Thus, the progeria protein remains intact with the nuclear envelope. Booth, L. (2012)

### 1.2.2 Progeria Protein

When the *LMNA* gene becomes mutated, usually but not always with a cytosine being replaced with an adenine, problems arise in the maturation process of the Lamin A protein. This single nucleotide mutation will cause an alternate splice site to appear. When this happens, during post-transcription processing of the messenger RNA (mRNA), a section of the gene is lost. Thus, during translation of the messenger RNA into protein, there is a missing sequence of 50 amino acids as compared to a healthy protein [10]. The region that is truncated contains the area that normally is attacked by proteases in the post-translational processing of the Lamin A protein, allowing the protein to disconnect them from the nuclear envelope [11]. Thus, the protein will fail to disconnect itself from the nuclear envelope. This mutated protein is called a progeria protein or a  $\Delta 50$  protein due to the missing 50 amino acids [Figure 1] [9].

### 1.3 Cell Physiology of Progeria

As noted, a healthy Lamin A protein will detach from the nuclear envelope and go on to help structure the interior of the nucleus [2] [5]. When the  $\Delta 50$  protein fails to detach from the nuclear envelope, it causes severe deformations of the envelope. Some of these deformations are seen as protrusions of the nucleus at odd angles. Another effect is that the  $\Delta 50$  stiffens the nucleus. When the nucleus becomes increasingly stiff, cells that are found in monolayers, such as endothelial cells, will be much taller and have varying responses to the mechanical stresses they are subjected to [11]. These taller cells could also have a shielding effect on surrounding cells [12].

Within the nucleus, it is believed that without the proper scaffolding in place, the condensation patterns of the nuclear material will change drastically [5] [8]. These patterns of condensation are believed to directly affect the transcription of specific genes and are responsible for making sure genes of higher importance to the cell, such as genes encoding proteins involved in respiration, are transcribed at a higher rate than others [12]. Yet, the nucleus is not the only place where alterations in the cell can be observed.

In cells with the  $\Delta 50$  present, there is an increase in the amount of reactive oxidative species (ROS). ROS can be responsible for many problems within the cell by creating free radicals that can hinder normal cell reactions. ROS are generally excreted from the cell [6]. If ROS are produced at a high enough rate, the cell will fail to keep up. They can cause problems including affecting the mitochondria. In normal cells mitochondria, the energy makers of the cell, will appear intact and string-like when viewed under a microscope [6]. Yet, when there is an increase in ROS, the mitochondria will go from long intact forms to highly fragmented and punctuated forms [Figure 2]. Generally, when the mitochondria go into this fragmented form, it is indicative that the cell is preparing to undergo apoptosis, or programmed cell death [7].

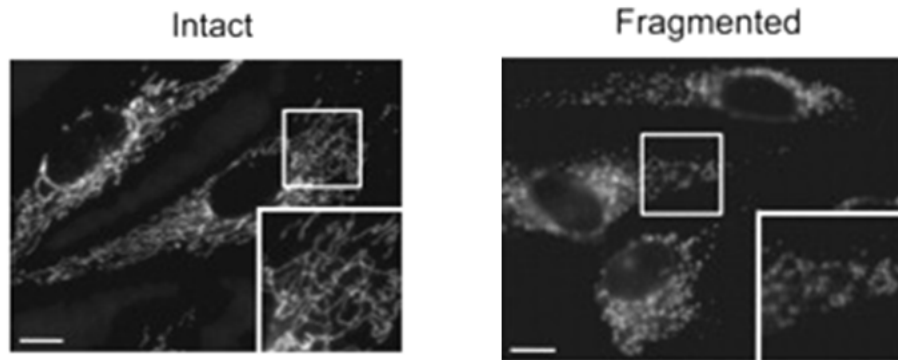


Figure 2: The differences in intact mitochondria and fragmented mitochondria. Notice how the intact mitochondria appear long and string-like whereas the fragmented ones are not. [7]

Cells with the  $\Delta 50$  have already been shown, using animal models, to have alterations in their expressions of mitochondrial proteins in response to shear stress [3]. Yet, no one has looked at this fragmented state of the mitochondria to determine how there is a link between a nuclear protein and the state of the mitochondria.

## 1.4 Image Analysis

To help determine how the mitochondrial structures and nuclear structures are linked in cells expressing the  $\Delta 50$  protein, I used image analysis techniques. These techniques include segmentation algorithms that are a combination of known and original ideas as well as different statistical and mathematical tools. In this section, I will be discussing the basis of the image analysis I used.

### 1.4.1 Imaging of Cells

After the endothelial cells were cultured, the cells were stained with fluorescent dyes in 3 channels. A channel in an image represents one of the three base colors: red, green, and blue. When an image is read in Matlab, it is read as a three dimensional matrix, with each dimension representing one channel. After staining the cells with

the three channels, they were imaged using fluorescent techniques. Fluorescent dyeing and imaging are generally easier to use than traditional RGB for many reasons. First, they provide clear detailed images of cells in channels that are easy to divide out and analyze separately. This is because the colors are very distinct and uniform. Also, intensity comparisons between cells becomes easier as all the same fluorophore is used throughout and will give off uniform amounts of fluorescence directly proportional to the amount present.

Fluorescent imaging is also useful in analyzing cells because it is highly specific. In staining the cells, a primary antibody is used to attach to the protein of choice. In my case, a protein found within the nucleus directly associated with all chromosomes, and a common mitochondrial protein were used. After the primary antibody attached, a secondary antibody attached to the primary antibody. This secondary antibody binding is highly specific to the primary antibody, and it can carry a multitude of fluorophores [14]. This technique of using a primary and secondary antibody is also useful in cutting costs. The primary antibodies are made specific to each protein being stained, yet the secondary antibody is made specific to all primary antibodies. Thus, one stock of secondary antibodies can service many primaries. This allows for very specific binding of the fluorophores [14].

Lastly, fluorescent imaging can provide detailed images without a lot of background. With normal light microscopes, you see everything within the cells. Even with oil techniques and other staining techniques, it is hard to eliminate background noise in the images. With fluorescence, the background noise is reduced greatly due to the specificity. Thus, detailed images of cells can be taken without having to look at more than one part of the cell at a time.

### 1.4.2 Segmentation

Image segmentation is a problem that many specialists in image analysis are trying to resolve. In this process, algorithms are designed that will identify the edges within an image, determine the important information in an image, and crop the image to only contain the important information. This is a challenge for many reasons. First, edge detection is an exceedingly difficult task to accomplish. The edges within an image are often blurred or not clearly defined. This is the case with the cells that I imaged. These cells were not stained for the cell membrane, so the mitochondrial material appears to be spread out in all directions. There are many techniques available to find edges, however, these techniques are specific to the type of images and stain used.

Secondly, segmentation is a problem in removal of background noises. Using a dye that is more specific can help with this, though no dye is perfect in eliminating background noise. The process of determining what is background noise can sometimes be difficult, though it is a vital in finding edges and determining junk information from useful information. Types of background can include washed out images where the fluorescence is turned up too high and a hue is present. An increase in fluorescence is also associated with photobleaching where the fluorophore loses its ability to fluoresce. Bits of lysed cells that are free floating but still contain some of the stain also need to be removed. All of these will cause problems later if not taken care of. This task is especially difficult in RGB where different colors are presented on a spectrum and not in nice neat channels and foreground information can often run into the background.

After the background noise is removed and edges have been detected, the next step is implementing a way to determine what information to keep. This part, in most segmentation algorithms I have seen, includes a user input to click in areas of interest. Included in this analysis is determining shape of the information to be segmented out. With shapes such as a nucleus, where things are generally round and uniform, determining important parts is easier. However, with images of whole monolayer

endothelial cells, the shapes are highly irregular, and the cells are often compacted close together. Thus, different techniques must be used to find the information to be analyzed.

Finally, segmentation of images is a time intensive project. Most images taken of cells are large files and there are hundreds that need to be taken into account. Thus, it takes a very long time to process each and every image individually, as there is universal process available.

### **1.4.3 Analysis**

After the images had been segmented and saved, individual cell images were analyzed. The analysis of the cells will be described in greater detail later.

## **1.5 Overview of Project**

The goal of my project was to develop techniques to analyze mitochondrial and nuclear textures to determine how they are different in HGPS patients as compared to healthy cells. Specifically, I investigated how these cells responded differently to shear stress, a type of mechanical stress found in the blood vessels. To do this comparison I developed a way to segment the mitochondrial and nuclear material.

# **2 Materials & Methods**

## **2.1 Cell lines**

Cell lines directly from HGPS patients were gathered from the Progeria Foundation Fibroblast. Procedures for thawing and preparing the cells were given by the Progeria Foundation protocols. The cells from the patients were positive for the mutation in exon 11 where cytosine was replaced with a thymine. These cells were grown in PBS solution and subcultured whenever confluency reached around 70%.

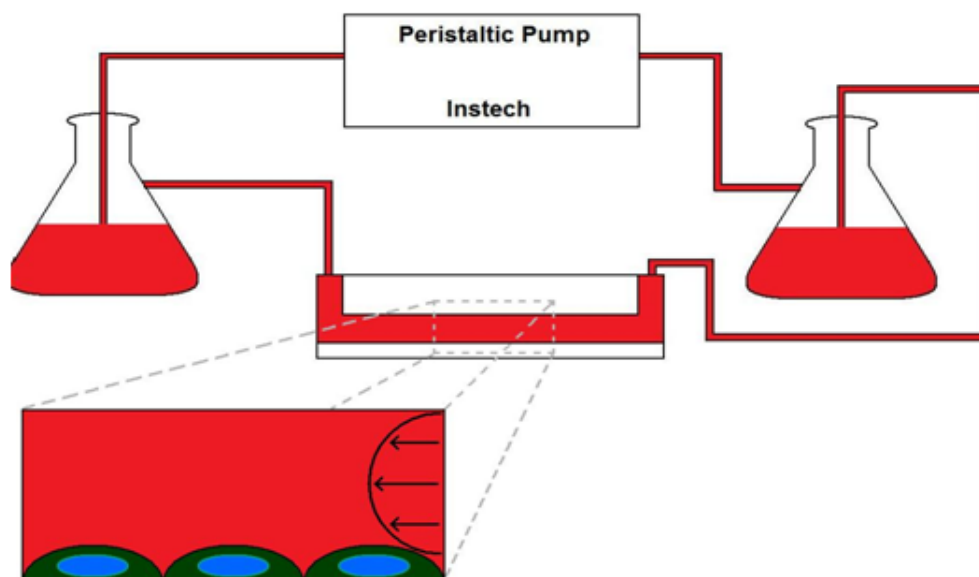


Figure 3: Diagram of the shear stress apparatus. The peristaltic pump allows for control of the amount of stress applied to cells ( $0 \text{ dyn/cm}^2$ ,  $5 \text{ dyn/cm}^2$ ,  $10 \text{ dyn/cm}^2$ ). The cells were placed in the bottom section and stress was applied. When imaging the cells, all images are oriented with stress going from the bottom to the top. Booth, E. (2012)

For the bulk of the analysis, human umbilical vein endothelial cells (HUVEC) were used. The cell lines used were ATCC Number: CRL-1730. Some of the cells were then transfected using lipofectin. The protocol for transfection was based on lipofectin basic techniques. Time for transfection was kept between 4-6 hours to minimize cell death. The cells were then cultured in PBS media and grown until confluent. The cells were subcultured when they reached 70% confluency.

## 2.2 Application of Shear Stress

After the cells were grown in culture, varying amounts of shear stress were applied to the cells. To do this, a monolayer of cells grown on a slide were placed in a shear stress apparatus [Figure 3]. This allowed for varying times (0 mins, 30 mins, 1 hr, and 6 hr) of stress to be applied. It also allowed for varying amounts of shear stress:

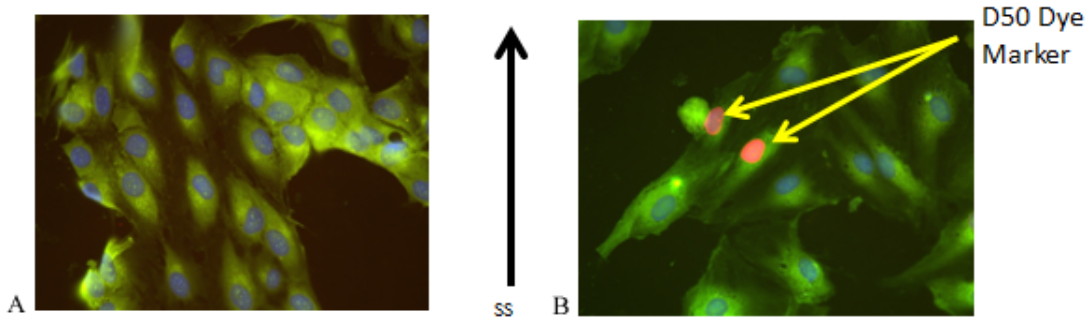


Figure 4: HUVECs after imaging. A) Control HUVEC with the JC-1 stain after high shear stresses for 1 hour. B) D50 HUVEC cells with the JC-1 stain, after high shear stress for 1 hour. The D50 Dye Marker is clearly marked and makes the nuclei appear pink. The arrow marked SS shows the direction of shear stress.

none (control), low (5 dyn/cm<sup>2</sup>), and high (10 dyn/cm<sup>2</sup>).

### 2.3 Staining and Imaging

After applying shear stress to the cells, HUVECs were stained using a JC-1 ratiometric fluorescent dye. The JC-1 was used to stain the mitochondria and is commonly used in apoptosis studies as healthy mitochondria will fluoresce green and unhealthy will fluoresce red. The nucleus was stained using a Hoechst stain. This made the nuclear material appear blue. A third D50 dye marker was used in the HUVECs to easily identify which cells had been properly transfected. This dye would attach specifically to the  $\Delta 50$  protein and fluoresce red. The combination of the D50 marker dye and the Hoechst made the nucleus of transfected cells appear pink.

The HGPS patient cell lines were stained for nuclear material only. For this, a DAPI stain was used. The DAPI will fluoresce green and is specific to condensation of nuclear material.

After staining, the cells were imaged on a Leica DMI 6000B Fluorescence and Light Microscope with the direction of stress from the bottom of an image to the top [Figure 4].

## 2.4 Segmentation of Images and Processing

Following microscopic analysis, the cell images were imported into Matlab. Then, using the Image Analysis Toolbox in Matlab, segmentation algorithms were developed to segment out the cells of interest. These cells were then saved into folders representing the different masks and channels. After the cells were saved, analysis of the mitochondrial texture was performed using an analysis program developed by Wei Wang of the Bioimage Informatics department at Carnegie Mellon University. This program used Linear Optimal Transportation (LOT) and Principal Component Analysis (PCA) to determine the largest differences between the cells. Finally, ratio statistics were run on the cells themselves to determine the ratio of red to green.

### 2.4.1 Development of the Segmentation Algorithm

Image segmentation is a difficult task. Especially with the HUVEC, getting rid of background noise, unwanted cells, and finding a cell mask that collects data for just the mitochondria was challenging [Figure 5].

The segmentation process that was developed involves a multi-step process. The first step involves taking the images and removing the background noise. To do this, a Gaussian blur technique was used. Blurring is a technique used in image analysis to make the images have harder edges. Specialized blurring algorithms, such as the Gaussian blur and tophat, are easily reversible and make it easier to use Matlab to understand the information present in the image. After the blur, a threshold level was set using a single domain histogram. After setting the threshold, the image was saved at the new threshold to eliminate background.

The next challenge was edge detection within the image. To find an edge, Matlab has to be able to determine where the cell border is. This provides a challenge as the mitochondria are not clearly marking the plasma membrane of the cells. Thus, in determining the edge, a tophat analysis was performed to create mountains of

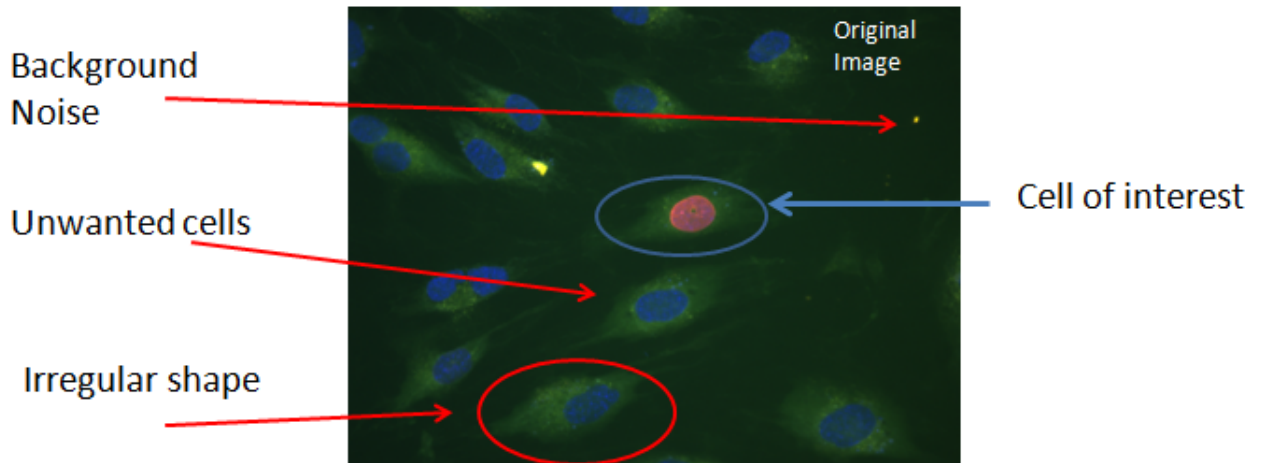


Figure 5: Problems that need to be overcome by segmentation. It can be seen that many pieces of background noise must be eliminated, the cells are closely compacted together with irregular shapes, and especially in the images with the transfected  $\Delta 50$  markers, only a few cells are of interest.

information. Each mountain represented a cell with intensities increasing as you traveled towards the nucleus. Then watershed lines were created. These watershed lines create an edge between cells. To make them, Matlab looked over the tophat image and determined where local maxima were and then found local minima between the maxima. It then connected all the local minima with white pixels. After the watersheding was complete, we could use Matlab to collect RegionProps on each encompassed area. These RegionProps are values such as maximum and minimum intensities, area, major and minor axis lengths and orientation, center locations, and assigned cell number.

After the initial analysis was performed, user input was required to select the cells of interest. It involved loading the images in a file and saving only those cells (encompassed by watershed lines) that the user needs. In the images with the  $\Delta 50$  cells, selections for only those cells with the D50 stain were selected. In the other images, only those cells that were completely encompassed by the watersheding and not on the perimeter of an image were used. After cell selection, the cell mask was

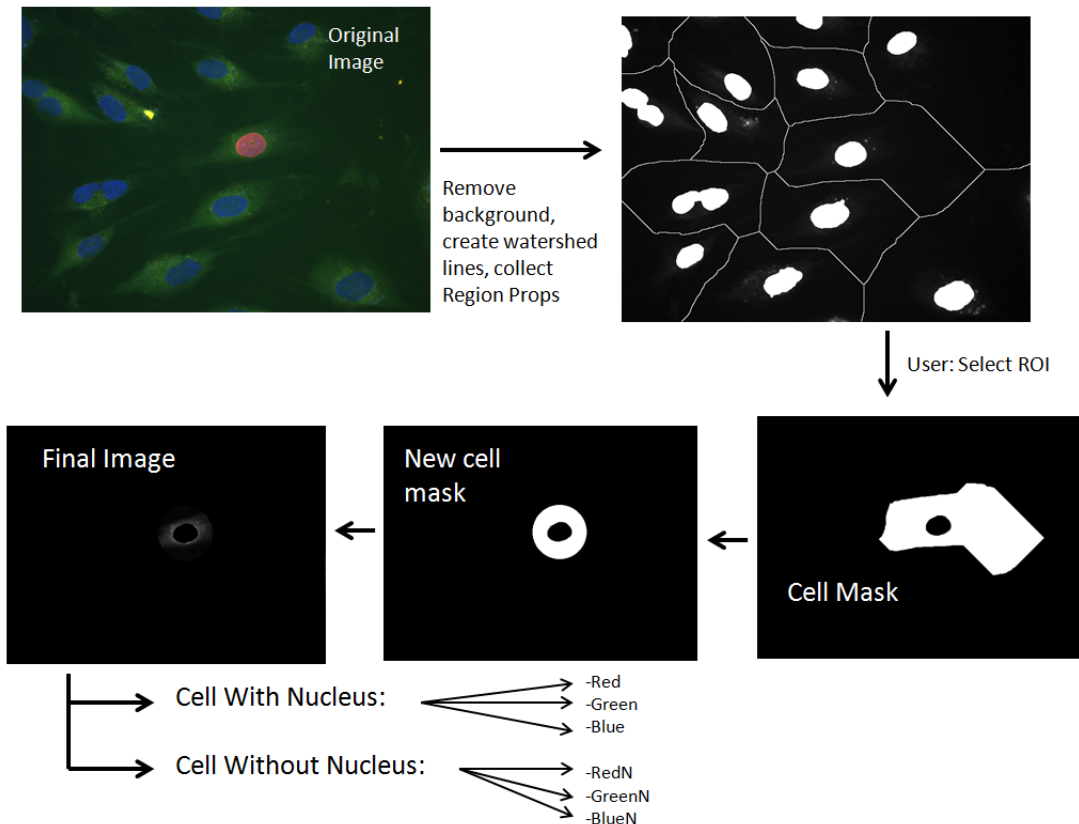


Figure 6: Outline of the segmentation of the HUVEC cells. From the original image, the background was removed, watershed lines were created, and RegionProps were collected. Then the user selects the ROI from the watershed image. The mask from the ROI is saved, modified if desired, then overlaid onto the final image. These final images are then saved with and without the nuclear data into each of the three channels.

saved (with and without the nuclear data). This cell mask was then placed over the original image and wherever the mask was white, the image was saved. All of the black sections of the image are erased and just the cell remains. More code was written to create modified masks to perform further analysis, such as measuring mitochondrial activity a given distance from the nucleus. Once all the masks were made, they were overlaid onto the original image, and then saved into separate folders with the three channels: red (unhealthy mitochondria), green (healthy mitochondria), and blue (nuclear material). [Figure 6]

In the HUVEC cells, the nuclei were edited out using similar techniques on the blue

channel. This allowed for masks with and without the nucleus. On the actual HGPS patient cell lines, a nuclear segmentation was developed. This involved adapting code created by Cheng Chen from Bioimage Informatics department at Carnegie Mellon University to match our needs. Chen's code works well with images that have regular shapes, such as a nucleus. His code determined a base shape for segmentation and scanned the image to find more regions that follow that same shape. It then created a specific mask for that shape and saved the masks in a workspace. Adapting the code simply required allowing it to loop around for all the images in a given folder and then overlay the mask. This required aligning the centroids and expanding the mask to cover the whole image. The nuclear data was then saved in a separate channel.

## 2.5 Post Segmentation Analysis

After the segmentation process, statistical measurements were taken on the mitochondria. The first measurement was a ratio test to find the difference between red and green fluorescence. This gave the ratio between healthy and unhealthy mitochondria. To do this, images had to be standardized. This was achieved by finding the maximum intensity in the red and the green and then dividing the image elementwise by this mean. This allowed for photobleaching effects to be eliminated. After normalizing all the images, mean intensities on each cell were taken. After finding the mean value for each image, the data was collected in MatLab in a vector for green and red and the red/green ratio was calculated for each cell. Then, for each data set (low and high shear stress with 0 min, 30 min, 1 hr, 6 hr) the average red/green ratio was calculated. These were plotted to show how mitochondria responded to the shear stress.

The cells were also run through specialized code developed by Wei Wang to perform LOT and PCA analysis. This analysis generates the statistical significance for each cell set and also provides a visual of the largest difference between the two data sets.

Finally, the nuclear data was saved and further analysis was performed.

## 3 Results

### 3.1 Segmentation

The segmentation process for all cell images was performed. After extensive accepting and rejecting of cells, individual cell images were saved. Among the HUVEC control cells, around 250 individual cells were collected per amount of shear stress (none, low 5 dyns/cm<sup>2</sup>, high 10 dyns/cm<sup>2</sup>) per exposure time (0 mins, 30 mins, 1 hr, 6 hr). For the HUVEC  $\Delta$ 50 transfected cell lines, around 100 individual cells were collected per amount of shear stress per exposure time. Images of these cells were saved in the red (unhealthy mitochondria), green (healthy mitochondria), and blue (nuclear) channels. Because of the highly irregular shape of the cells and varying masks created with the watershed lines, circular masks were also created for each cell image centered on the nucleus. These were then saved in all three channels. Thus, for every cell, there were 6 different images from which data could be collected: red, green, and blue with the cell mask and red, green, and blue with the circular mask. The nuclear data was then saved into a separate location.

The RegionProps for the cells was also collected. This information was saved per cell and contained data for the red, green, and blue channels. The RegionProps for each cell also contained the information for the nuclear data. The individual cell image names were formatted as such: ImageXXX\_YY. The XXX represented the image number and YY was the cell number on that original image.

From the patient cell lines, the nuclear segmentation information was saved in just the green (DAPI) channel used to stain the patient nuclei. From these cells, we obtained around 300 nuclei per HGPS patient and 200 per healthy patient.

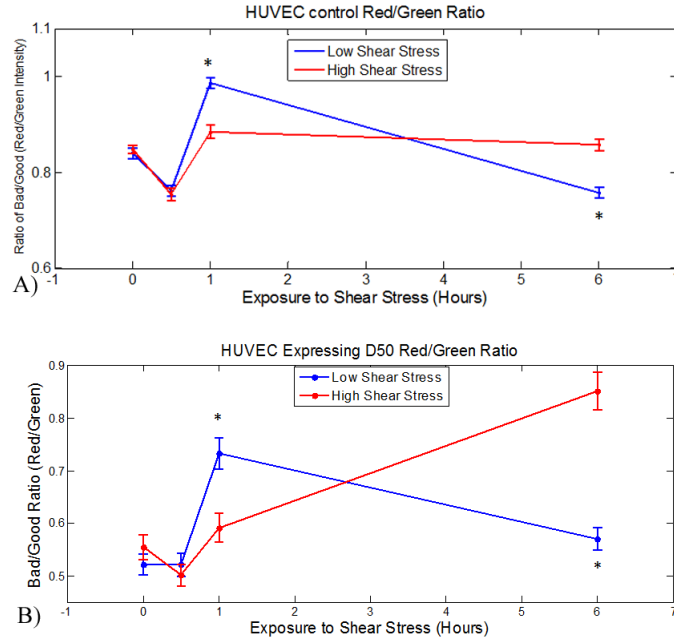


Figure 7: Results of the red/green ratio comparisons in HUVECs. A) Response of HUVEC control cells to shear stress. With low shear stress there is an increase in the amount of bad mitochondria at one hour but a significant decline between one and six hours. The high shear stress cells appear to be relatively constant between one and six hours. The intervals contain 95% confidence. B) Response of HUVEC with  $\Delta 50$  to shear stress. An increase at one hour can be seen with a decline to six hours. However, in the high shear stress, there appears to be a gradual increase to the six hour time point.

### 3.2 Ratio Results

The basic red/green ratio tests were run comparing HUVEC and HUVEC with  $\Delta 50$  under low and high shear stress [Figure 7]. A few interesting results came from the ratio tests. The first is that in all cell lines, there is a large spike in the red/green ratio at one hour. After the spike, all cell lines show a decline at the six hour time point in the red/green ratio back to original levels. In the HUVEC control cell lines, under high shear stress there is no real difference between one and six hours. There is a decline beginning at 30 minutes but a return to normal levels by 6 hrs. In the HUVEC with  $\Delta 50$ , this is not the case. The cells of this line show the decline beginning at 30 minutes and a return to normal levels at one hour. Yet, at six hours there is a large

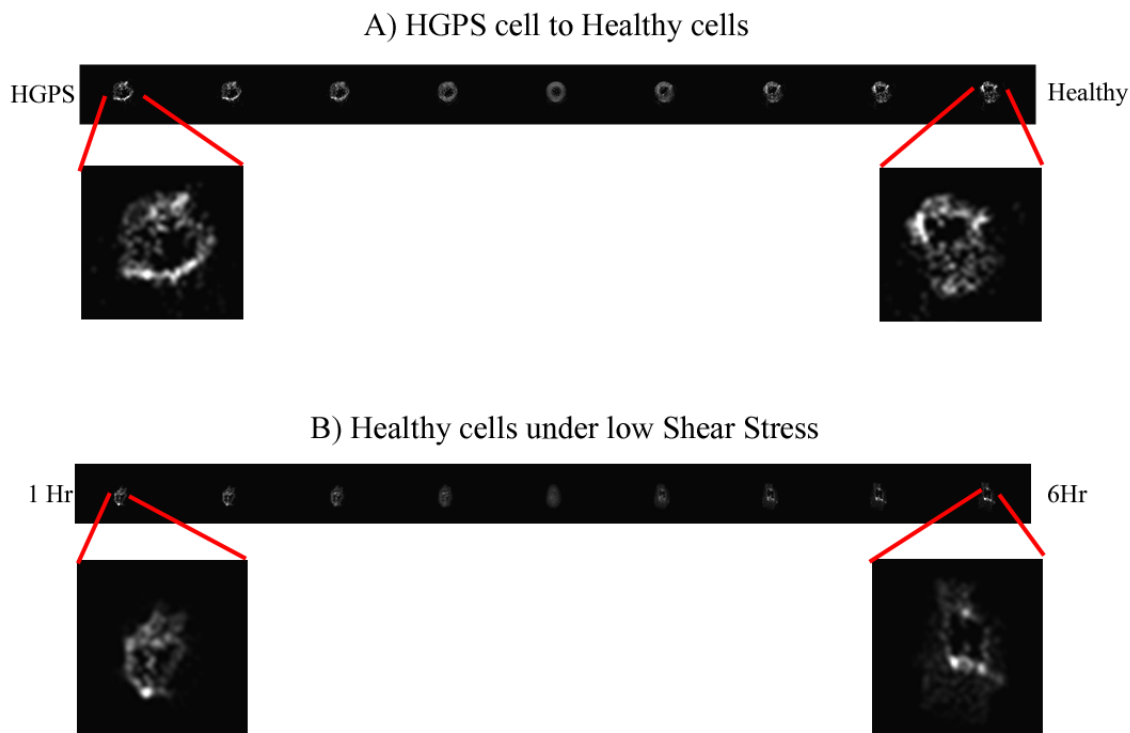


Figure 8: Results of the LOT comparison. A) Comparison of the HGPS cells to healthy cells with respect to mitochondrial textures. The end cells are the averages for each cell type. The largest calculated difference is shown. B) Showing the same thing for healthy HUVEC cells under shear stress for one hour as compared to six hours. All images were in the red (unhealthy mitochondria) channel.

increase in the red/green ratio implying there are more unhealthy mitochondria. All data was collected with 95% confidence.

### 3.3 LOT and PCA Analysis

The results from the LOT and PCA analysis on mitochondrial texture can be seen in Figure 8. These results are showing the LOT calculated after the PCA. For this analysis, we only included the biggest calculated difference. On the endpoint images, the averages for the specified cell types are shown. For example, in Figure 8A we see the average for mitochondrial texture in the HGPS cells on the left and the average for the mitochondrial texture for the healthy cells line on the right. Then the shortest distance morphology from one average to another is shown looking across from left

to right. The end points have been blown up to accentuate the differences. Both differences had  $p < 0.05$ .

In the HGPS cells compared to the healthy cell lines, there was a notable difference in the clumping of the mitochondria. In the HGPS cells, we see large clumps of mitochondria right next to the nuclei. In the healthy cell lines, we see fewer large clumps of mitochondria and the spread is further from the nucleus. When looking at the healthy cells under low shear stress, at one hour there is hardly any clumping of the mitochondria and they appear to be healthy. Yet, after six hours, we see only a few large clumps of mitochondria very close to the nucleus.

## 4 Discussion

From the work done on these cells, large amounts of data on many different cell types with varying amounts of shear stress applied was collected. Also, a lot of statistical data on mitochondria health and texture was collected. Finally, ample amounts of nuclear data were collected to perform further testing.

### 4.1 Segmentation Algorithms

The segmentation algorithms designed or adapted for the image analysis worked pretty well. I was able to process about 75 cells per hour. We did have to throw out many cells because they were too close to the edge of an image or the watershed-ing was not working properly on them. This could create a potential bias because it was all left to the discretion of the user to determine which cells to keep and which to toss. To keep things as unbiased as possible, as many cells as possible were collected. Also, from a single slide of cells, multiple sets of images were taken to ensure that as many whole cells as possible were present.

The segmentation process had a few other issues. It tended to create highly ir-

Cell Mask without Nucleus

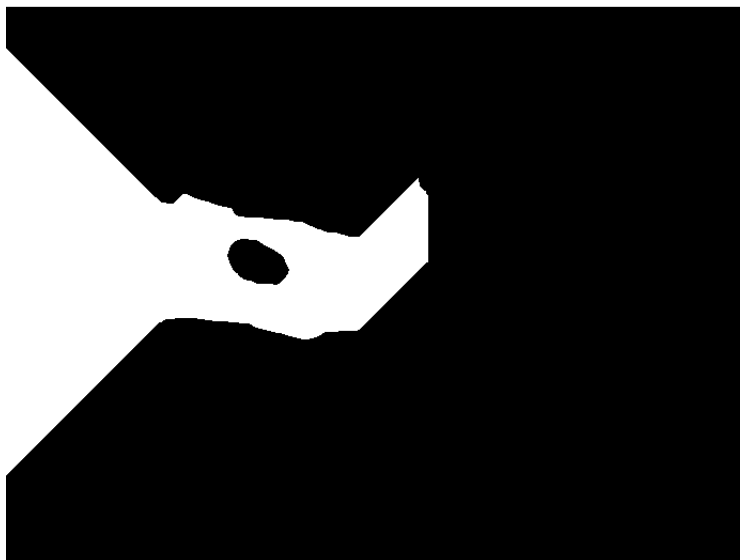


Figure 9: Example of a cell mask located near the edge of an image. Notice how the mask tends to spread as it gets closer to the edge. Most of these images had to be discarded when performing the LOT analysis.

regular cell shapes that were not fully indicative of the true cell shape. Having the ability to smooth out the lines created after watersheding would help with the problem. Strange cell shapes became an issue when performing the LOT transformation. Initially, due to the highly irregular cell shapes, the LOT was always saying that cell shape was the largest difference. To compensate for this, all cells at the edge of an image were thrown out from the LOT analysis. These cells tended to have watershed lines that spread the closer they got to the image edge [Figure 9].

The circular masks were used to make measurements a set distance from the nucleus. The segmentation code allowed for the option of producing a circular mask or not as well as setting the radius of the circle. It used a simple equation for a circle to make one of the given size and align its centroid with that of the cell nucleus. This also helped with the issue of irregular cell shape. By standardizing the shape of the mask it made the segmentation easier. With the circular mask, there were a few problems. The first was because the cells were confluent. Confluent cells are tightly

packed together and do not leave a lot of space between the nuclei. Often, confluent cells are so narrow along the minor axis, there is only a few pixels of information between the nucleus and cell membrane. When a circle was overlaid on a cell with a large difference between the major and minor axis, crossing over into another cell along the minor axis often occurred. We saw this happening and in the LOT analysis; halos would form around the edges. For this reason, with the circular mask more cells had to be discarded if they were too close to their neighbor. To compensate for this, an elliptical mask is in development that would align with the major axis of the cell image.

The nuclear segmentation algorithm worked really well. This was easier material to segment and pre-established algorithms were available to adapt to our specific needs. Thus, this data provided lots of information with fewer images. This was especially good because we had fewer cell lines to work with when it came to the patient cells. The only real problem was nuclei located at the edge of an image. If there was any missing information from the nucleus, the program would sometimes still detect the nuclear information. When this happened, manually discarding the partial nuclei was required.

## 4.2 Ratio Tests

The results from the ratio tests were a little surprising. The spike in the ratio of red/green (unhealthy/healthy mitochondria) under low shear stress in both the control HUVECs and the  $\Delta 50$  HUVECs was unexpected. This implied that after only one hour under low shear stress, cells were starting to be affected. Yet, in both cases, a return to normal levels was seen. This implies that the cells between one and six hours are repairing themselves. Possible reason from this could be that the cells actually are repairing themselves, or that the cells that could not repair themselves were dying between one and six hours.

The high shear stress results were as expected. The large spike at six hours in the  $\Delta 50$  cells was as expected. This follows with previous research that shows mitochondrial proteins differ greatly in response to high shear stress. To really understand what is happening, more data points between one and six hours need to be taken, as that is where the differences in expression are seen.

### 4.3 LOT Analysis

The LOT analysis provides insight into the behavior of the mitochondria as compared to the state of the mitochondria that was seen with the ratio tests. The mitochondria were seen to show different textures as was expected. The more interesting result was the comparison of the one to six hours in the control HUVECs. At these two time points, the one hour stress treatment showed a large increase in the ratio of red/green fluorescence that then returned to normal levels after six hours. By looking at the LOT a possible reason for this change can be seen. At one hour, the red channel of the mitochondria is much more intense and clumped. Yet, by hour six, the mitochondria in the red channel are almost completely gone except for a large clump right next to the nucleus. There are two possible explanations for this. First is the large amount of unhealthy mitochondria seen at one hour are dying between one and six hours and thus are no longer able to carry the proteins the fluorescent tags are attaching to. Second could be that the mitochondria may be repairing. This would greatly decrease the amount of red fluorescence.

When looking at the red channel with the HGPS patient cells and the healthy cells, the difference is only in the distribution of mitochondria away from the nucleus. This distribution difference suggest the the mitochondria, when coming into a pre-apoptosis state, have a higher tendency to clump together. This clumping could prevent enzymes specific to waste disposal from getting to these unhealthy mitochondria and could be creating a toxic environment in the cells. Further testing is needed

to make any strong conclusions about mitochondrial behavior, including taking even higher quality images to determine if the mitochondria are clumping or fusing.

## 5 Conclusion

This work is a good stepping stone into further analysis of the mitochondrial texture and nuclear texture in HGPS cells. Development of a segmentation process is an important step because it will allow for large data sets to be analyzed in a much shorter amount of time. Though it is still not perfect, the algorithm I designed was able to drastically cut down on time to isolate individual cells for comparison. More techniques could be developed to cut down on time and be more efficient, including an elliptical mask to overlay on the confluent cells along their major axis. Also, finding ways to eliminate the user input sections would make things a lot faster and help eliminate human bias. Both are important in future work on the algorithms.

The ratio tests performed provided a lot of data. Yet, more is needed. This was a good starting point as we now know that big differences are happening between one and six hours. We also know that doing similar analysis with multiple time points in the range is needed to better understand what is happening. To help with better understanding of the ratio results, more LOT analysis should be performed. Currently, with the number of cell images being used and the size of the images, running one PCA and LOT analysis takes a full day. Future comparisons to be run include comparing the low shear stress  $\Delta 50$  cells between one and six hours, the low shear stress at six hours between  $\Delta 50$  and healthy cells, and the high shear stress  $\Delta 50$  cells between one and six hours. These would provide a lot more information about not only the state the mitochondria are in (as with the ratio tests) but the behavior of the mitochondria. Combining state and behavior can help to develop a full model of the changes in mitochondria texture in response to shear stress.

Other future work that could be done is running analysis programs on the nuclear data. The intended next step for the nuclear data is to perform LOT analysis to determine differences in condensation patterns. Performing intensity comparisons would help to understand how this is changing the nucleus. This nuclear data is vital in trying to bridge a nuclear protein to changes in mitochondria.

Lastly, shielding effects could be measured. The nuclei of the  $\Delta 50$  cells are not only stiffer but more elevated. This makes the cell, which is normally rather flat, have a taller presence as compared to the cells around it. It has been hypothesised that these  $\Delta 50$  cells will shield their neighbors. Thus, comparing downstream and upstream cells from those transfected could provide information about whether or not shielding is causing a difference in the mitochondria behavior. To take this the next step, better imaging of the mitochondria to determine if they are clumping or combining could be done. This would be interesting because if the mitochondria are combining, then excreting them from the cell would be more difficult and the mitochondria would create a toxic environment.

## 6 Acknowledgments

I would like to thank Dr. Kris Dalh and the Dahl Labs at Carnegie Mellon University for taking me in during the summer and allowing me to do this research. Specifically I would like to thank Dr. Libby Booth and Steve Spagnol for mentoring me in the computer programming and sterile lab techniques. I would like to thank the TECBio REU program funded through the NSF for the funding to do this project. At Carroll College, I would like to thank Dr. Kelly Cline for being my thesis advisor and Dr. Stefanie Otto-Hitt, Dr. Virginia Cooper, and Phil Rose for being on my reading committee. Finally, I would like to thank my Mom and Dad and whole family for their support.

## References

- [1] Dechat, T. et al. *Nuclear lamins: major factors in the structural organization and function of the nucleus and chromatin*. Genes & Development vol. 22: 832-853 2008.
- [2] Jammerding, J. et al., *Lamins A and C but Not Lamin B1 Regulate Nuclear Mechanics*. Jour. Biol. Chem. vol. 281 no. 35: 25768-25780 Sept. 2006.
- [3] Fisher, A.B. Chien, S. Barakat, A.I. Nerem, R.M., *Endothelial cellular response to altered shear stress*. Am J Physical Lung Cell Mol Physiol vol. 281: 529-522 2001.
- [4] Chatzizisi, Y.S. Coskun, A.U. Jonas, M. Edelman, E.R. Feldman, C.L. Stone, P.H. *Role of Endothelial Shear Stress in the natural history of Coronary Atherosclerosis and Vascular Remodeling*. Jor. American College of Cardiology vol 49 no.25 2007.
- [5] mounkes, L.C. Stewart, C.L. *Aging and nuclear organization: lamins and progeria*. Current Opinion in Cell Biology vol. 16: 322-327 2004.
- [6] Papapetropoulos, A. Garcia-Cardena, G. Madri, J.A. Sessa, W.C. *Nitric Oxide Production Contributes to the Angiogenic Properties of Vascular Endothelial Growth Factor in Human Endothelial Cells*. J. Clin. Invest. vol 100 no.12: 3131-3139 1997.
- [7] Geidt R.J. et al *Mitochondrial fusion in endothelial cells after simulated ischemia/reperfusion: role of nitric oxide and reactive oxygen species*. Free Radical Biology Medicine 52, no. 2: 348-56 2012.
- [8] Mattout, A. Dechat, T. Adam, S. Goldman, R.D. Gruenbaum, Y. *Nuclear lamins, diseases and aging*. Current Opinion of Cell Biology vol. 18:335-341 2006.

- [9] Dahl, K.N. Scaffidi, P. Islam, M.F. Yodh, A.G. Wilson, K.L. Misteli, T. *Distinct structural and mechanical properties of the nuclear lamina in Hutchinson-Gilford progeria syndrome*. PNAS vol. 103 no. 27:10271-10276 2006.
- [10] Glynn, M.W. Glover, T.W. *Incomplete processing of mutant lamin A in Hutchinson-Gilford progeria leads to nuclear abnormalities, which are reversed by farnesyltransferase inhibition*. Human Molecular Genetics vol. 14 no. 20:2959-2969 2005.
- [11] Mounkes. L. Kozlov, S. Burke, B. Stewart, C.L. *The laminopathies: nuclear structure meets disease*. Current Opinion in Genetics & Development vol 13: 223-230 2003.
- [12] Broers, J. LV. Hutchison, C.J. Ramaekers, F. CS. *Laminopathies*. Jour, of Pathol vol 204: 478-488 2004.
- [13] Wang W, et al. *A linear optimal transportation framework for quantifying and visualizing variations in sets of images*. Unpublished 2012.
- [14] JC-1 Dye- Mitochondrial Membrane Potential Probe *Life Technologies*. July 13 2012 <http://www.invitrogen.com/>.